**SUPLEMENTARY FIGURES AND TABLES**

# Rapid affinity optimization of an anti-TREM2 clinical lead antibody by cross-lineage immune repertoire mining


**AUTHORS**

Yi-Chun Hsiao[1], Heidi Ackerly Wallweber[2], Robert G. Alberstein[3], Zhonghua Lin[1], Changchun Du[4], Ainhoa Etxeberria[5], Theint Aung[1], Yonglei Shang[1,6], Dhaya Seshasayee[1], Franziska Seeger[3], Andrew M. Watkins[3], David V. Hansen[5,7], Christopher J. Bohlen[5], Peter L. Hsu[2], Isidro Hötzel[1#]

[1]Department of Antibody Engineering, Genentech, South San Francisco, CA 94080, USA. [2]Department of Structural Biology, Genentech, South San Francisco, CA, USA. [3]Prescient Design, a Genentech Accelerator, South San Francisco, CA, USA. [4]Department of Biochemical and Cellular Pharmacology, Genentech, South San Francisco, CA, USA. [5]Department of Neuroscience, Genentech, South San Francisco, CA, USA.

[#]e-mail: ihotzel@gene.com

[6]Current address: Amberstone Biosciences, Irvine, CA, USA

[7]Current address: Department of Chemistry and Biochemistry, Brigham Young University, Provo, UT, USA

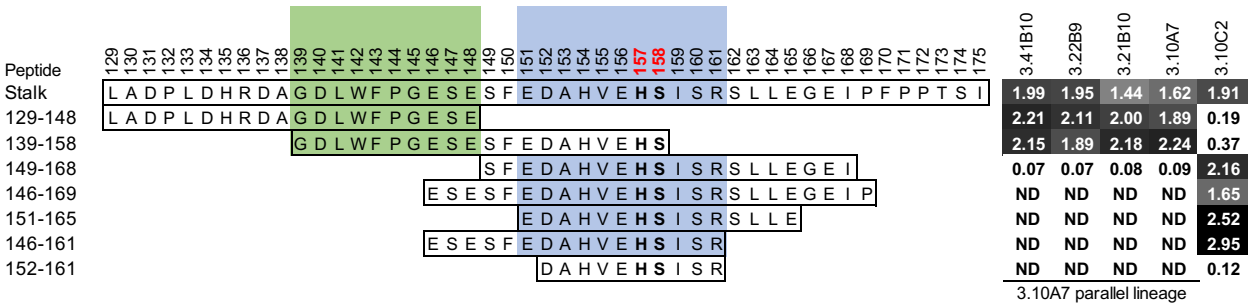


**Supplementary Fig. 1 Mapping of epitopes bound by anti-TREM2 antibodies.** Overlapping peptides corresponding to the TREM2 stalk region were used in ELISA to test antibody binding. Sequences of peptides are shown with the presumed approximate boundaries of the epitopes bound by antibodies of the 3.10A7 parallel lineage group and antibody 3.10C2 highlighted in green and blue, respectively. Values shown are raw ELISA $OD_{450}$ readings, highlighted proportionally to intensity. The ADAM10/17 cleavage site is highlighted in red. ND, not done.

a

| Antibody | ka (1/Ms) | kd (1/s) | KD (M) |
|---|---|---|---|
| 3.10A7 | 7.7E+05 | 7.8E-04 | 1.0E-09 |
| 3.21B10 | 3.0E+05 | 1.6E-04 | 5.4E-10 |
| 3.22B9 | 1.6E+05 | 2.5E-04 | 1.6E-09 |
| 3.41B10 | 4.9E+05 | 2.4E-03 | 4.8E-09 |

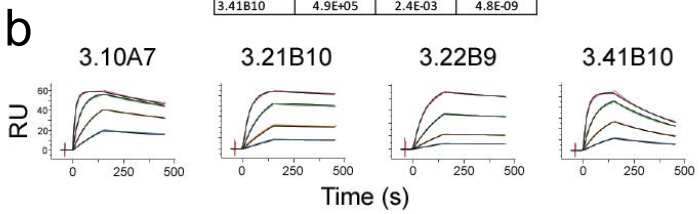


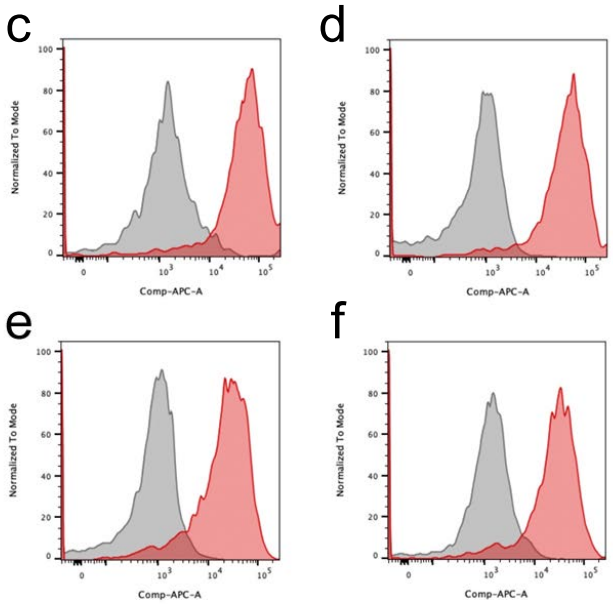


g

| Antibody | Rat | VH | VL | JH | JL | CDR H3 length | DH | DH segment sequence | DH segment reading frame | CDR H3 sequence | CDR H3 aa identity with Ab: 3.10A7 | 3.22B9 | 3.41B10 | Clonotype (by definition): Biological | Working |
|---|---|---|---|---|---|---|---|---|---|---|---|---|---|---|---|
| 3.10A7 | R18 | VH10-5 | VK8U89d | JH2 | JK4 | 11 | DH1-11 | ACTACGG | 1 | **TAGTT**VV--**PFDY** | | 82% | 27% | 1 | 1 |
| 3.22B9 | R18 | VH10-5 | VK8U89d | JH2 | JK5 | 11 | DH1-10 | ACAACTAC | 1 | **TAGTTT**A--**PFDY** | 82% | | 27% | 2 | 1 |
| 3.41B10 | R20 | VH10-5 | VK8U89d | JH3 | JK5 | 11 | DH1-11 | GAGGG | 1 | TGEGPQGG--FVY | 27% | 27% | | 3 | 3 |
| 3.21B10 | R18 | VH10-5 | VK8U89d | JH3 | JK5 | 13 | DH1-11 | TTAACTACGGAGGGT | 3 | IEGVNYGGSPFVY | 31% | 31% | 38% | 4 | 4 |

**Supplementary Fig. 2 Affinities, cell binding and clonotyping of clones in the 3.10A7 parallel lineage.** (a) Monovalent binding kinetics and $K_D$ of antibodies to TREM2 at 37ºC by SPR measured in a Biacore 8K instrument. (b) SPR sensorgrams corresponding to data in panel (a). Color and black lines are sensorgram data and curve fitting, respectively. TREM2 antigen used at 100 nM for the highest concentration followed by 3-fold dilutions. Binding of purified hybridoma antibodies (c) 3.10A7, (d) 3.21B10, (e) 3.22B9 and (f) 3.41B10 to Jurkat cells expressing TREM2 by flow cytometry. Gray, control IgG2a. Red, antibodies. Comp-APC-A, median fluorescence intensity of binding. (g) Clonotyping of the 3.10A7 group of clones. Parameters used for clonotyping are shown in columns 2 to 14, color-coded in each column for easier differentiation. Parameters shaded in gray are not used for the working clonotype definition. “Biological” and “Working” refer to clonotype classification using the biological or working clonotyping definitions. Sequence identity with the 3.21B10 clone is performed by inserting a gaps of two positions as indicated by dashes. Identical amino acid residues between clones 3.10A7 and 3.22B9 are highlighted in boldface. DH, IGHD segment. Complete junctional sequence parsing information is given in Supplementary Fig. 3.

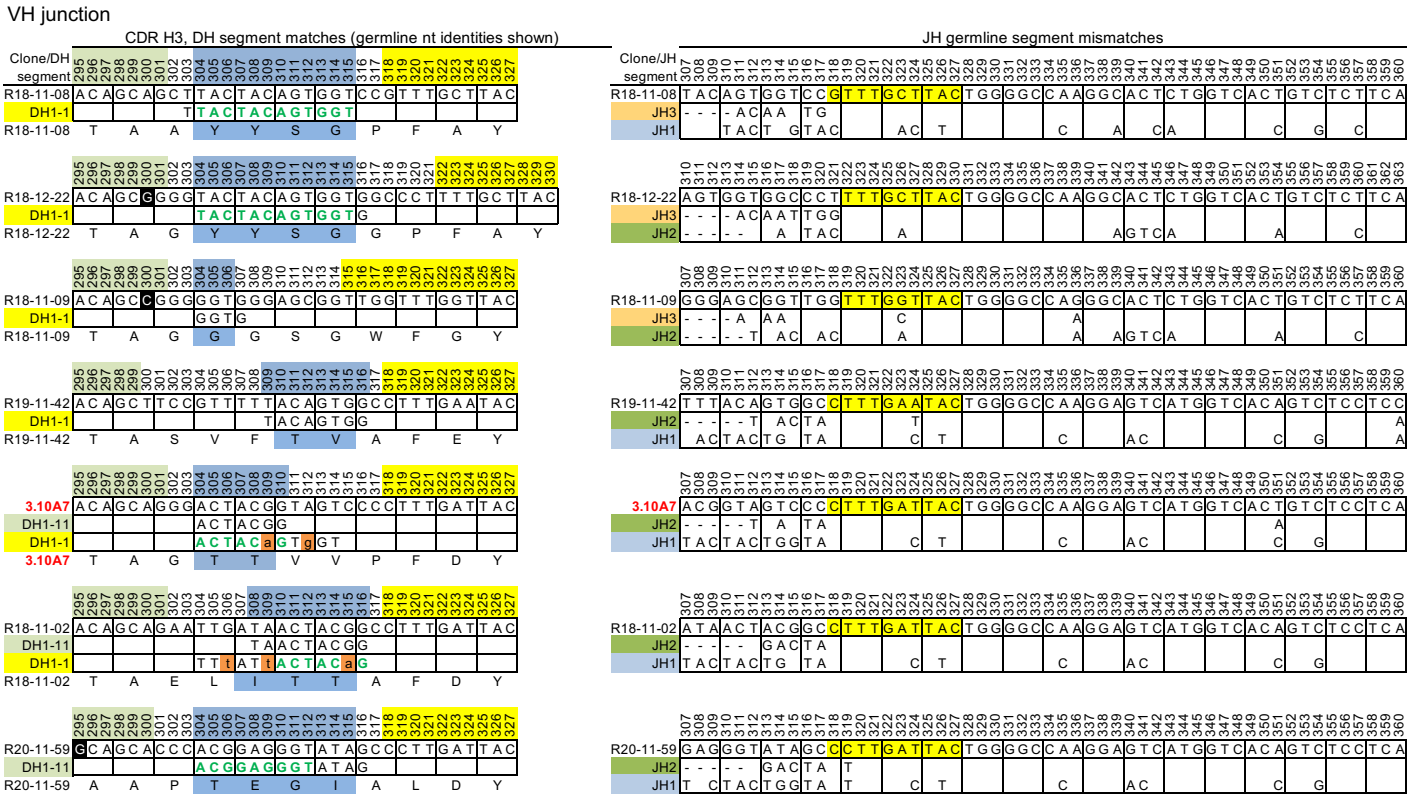


**Supplementary Fig. 3 Junctional sequence analysis of selected clones in the 3.10A7 and 3.10C2 parallel lineage groups.** The left column shows CDR H3 sequences with parsing information in colors above the sequences, in the $V_H$ nucleotide number row, for regions likely derived from $V_H$ (green), $D_H$ (blue) and $J_H$ (yellow) germline segments. The row below the antibody nucleotide sequence shows the DH region matches, with possible somatic mutations in lower case and highlighted in orange. For some CDR H3 sequences two possible matches are shown. CDR H3 amino acid residues encoded by at least two $D_H$ nucleotides within the codon are highlighted in blue. The $D_H$ germline segment names are highlighted in different colors for easier identification of CDR H3 sequences with the same likely $D_H$ segment. Similar $D_H$ sequences in the same reading frame in different clones (usually the previous or following clone) are highlighted in green. Nucleotides that differ from the ACAGCAG contributed by $V_H$10-5 to CDR H3 are shown in black backgrounds. The right column shows detailed parsing information for the top two $J_H$ hits with nucleotides in the $J_H$ germline segments identical the antibody not shown. The last 4 alignments show $J_L$ alignments for the hybridoma clones in the 3.10A7 parallel lineage and 3.10C2 clonotype groups. Dashes show regions not covered by the $J_H$ sequence. $J_H$ germline segment names are color coded for clarity. The region of $J_H$ included in CDR H3 is highlighted in yellow on the antibody sequences. Sequences are sorted by $D_H$ region in CDR H3. Names of hybridoma-derived clones are highlighted in red. Allele information is omitted for clarity. Figure continued in following pages. Note that the boundaries of $D_H$ and $J_H$ overlap in some clones and some $J_H$ boundaries are uncertain due to possible somatic mutations. Figure continued on pages 5 to 8.

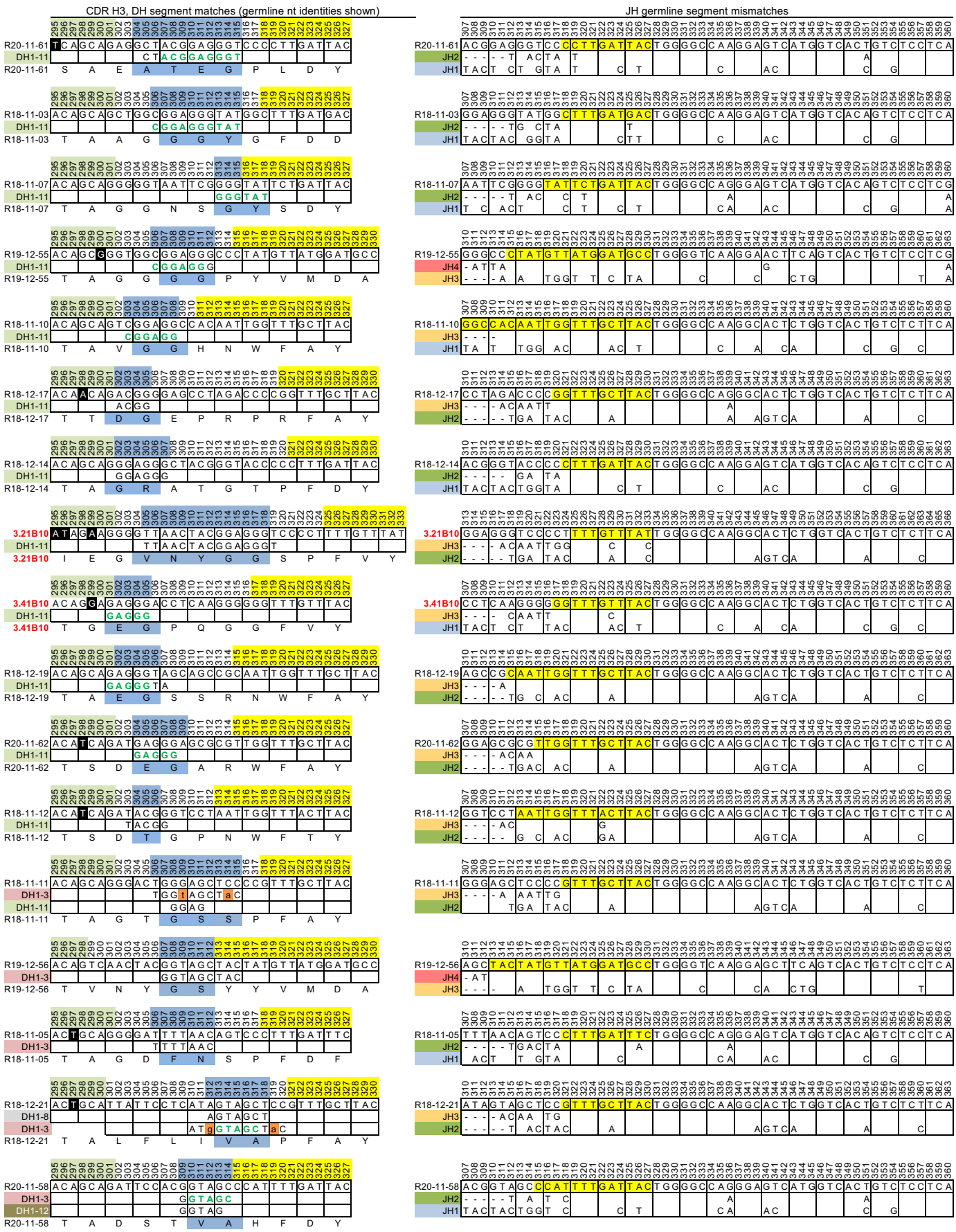
CDR H3, DH segment matches (germline nt identities shown)
JH germline segment mismatches
R20-11-61
DH1-11
R20-11-61
R18-11-03
DH1-11
R18-11-03
R18-11-07
DH1-11
R18-11-07
R19-12-55
DH1-11
R19-12-55
R18-11-10
DH1-11
R18-11-10
R18-12-17
DH1-11
R18-12-17
R18-12-14
DH1-11
R18-12-14
3.21B10
DH1-11
3.21B10
3.41B10
DH1-11
3.41B10
R18-12-19
DH1-11
R18-12-19
R20-11-62
DH1-11
R20-11-62
R18-11-12
DH1-11
R18-11-12
R18-11-11
DH1-3
DH1-11
R18-11-11
R19-12-56
DH1-3
R19-12-56
R18-11-05
DH1-3
R18-11-05
R18-12-21
DH1-8
DH1-3
R18-12-21
R20-11-58
DH1-3
DH1-12
R20-11-58
JH2
JH1
JH4
JH3

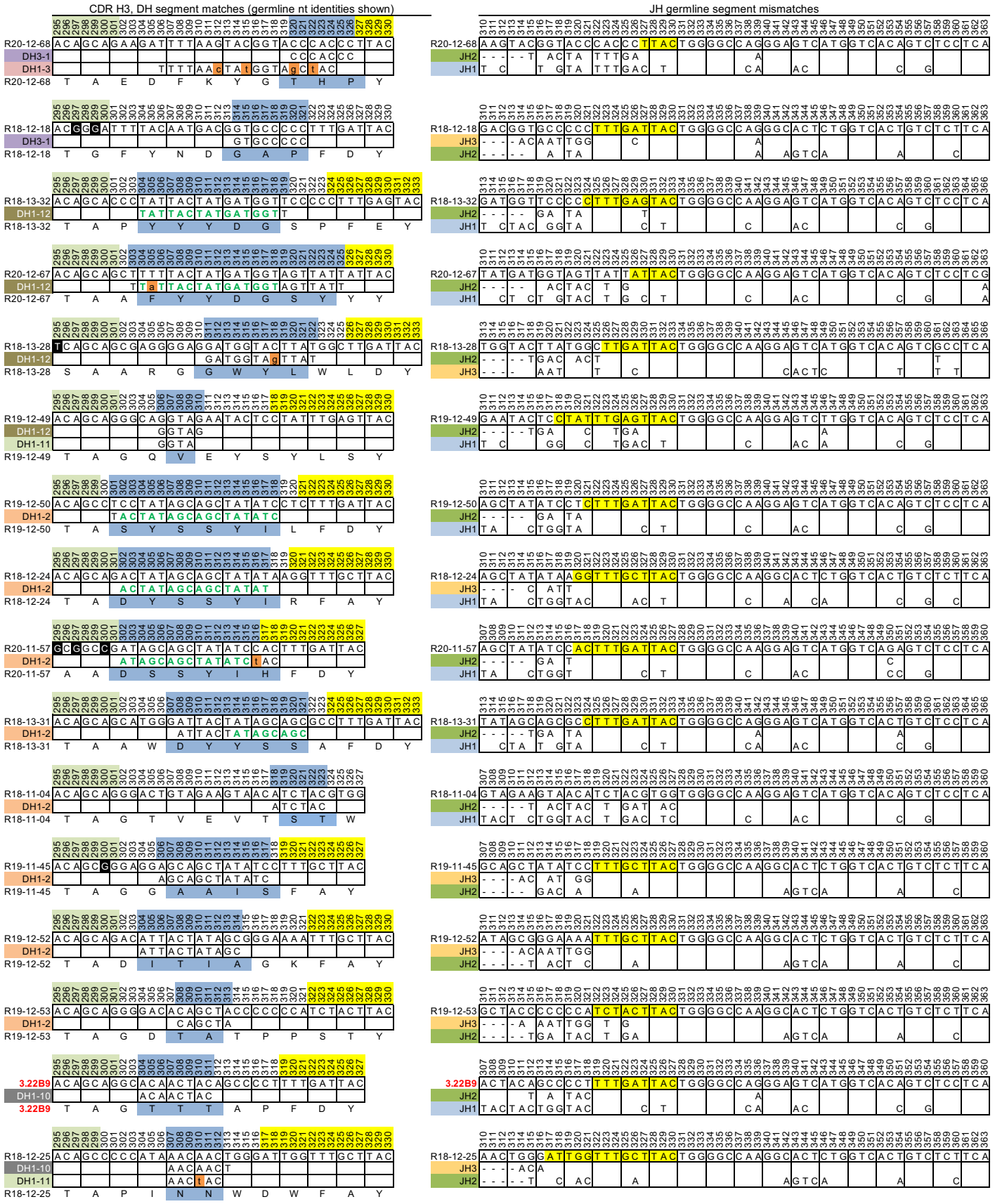
CDR H3, DH segment matches (germline nt identities shown)
JH germline segment mismatches
R20-12-68
DH3-1
DH1-3
R18-12-18
DH3-1
R18-13-32
DH1-12
R20-12-67
DH1-12
R18-13-28
DH1-12
R19-12-49
DH1-12
DH1-11
R19-12-50
DH1-2
R18-12-24
DH1-2
R20-11-57
DH1-2
R18-13-31
DH1-2
R18-11-04
DH1-2
R19-11-45
DH1-2
R19-12-52
DH1-2
R19-12-53
DH1-2
3.22B9
DH1-10
R18-12-25
DH1-10
DH1-11
JH2
JH1
JH3

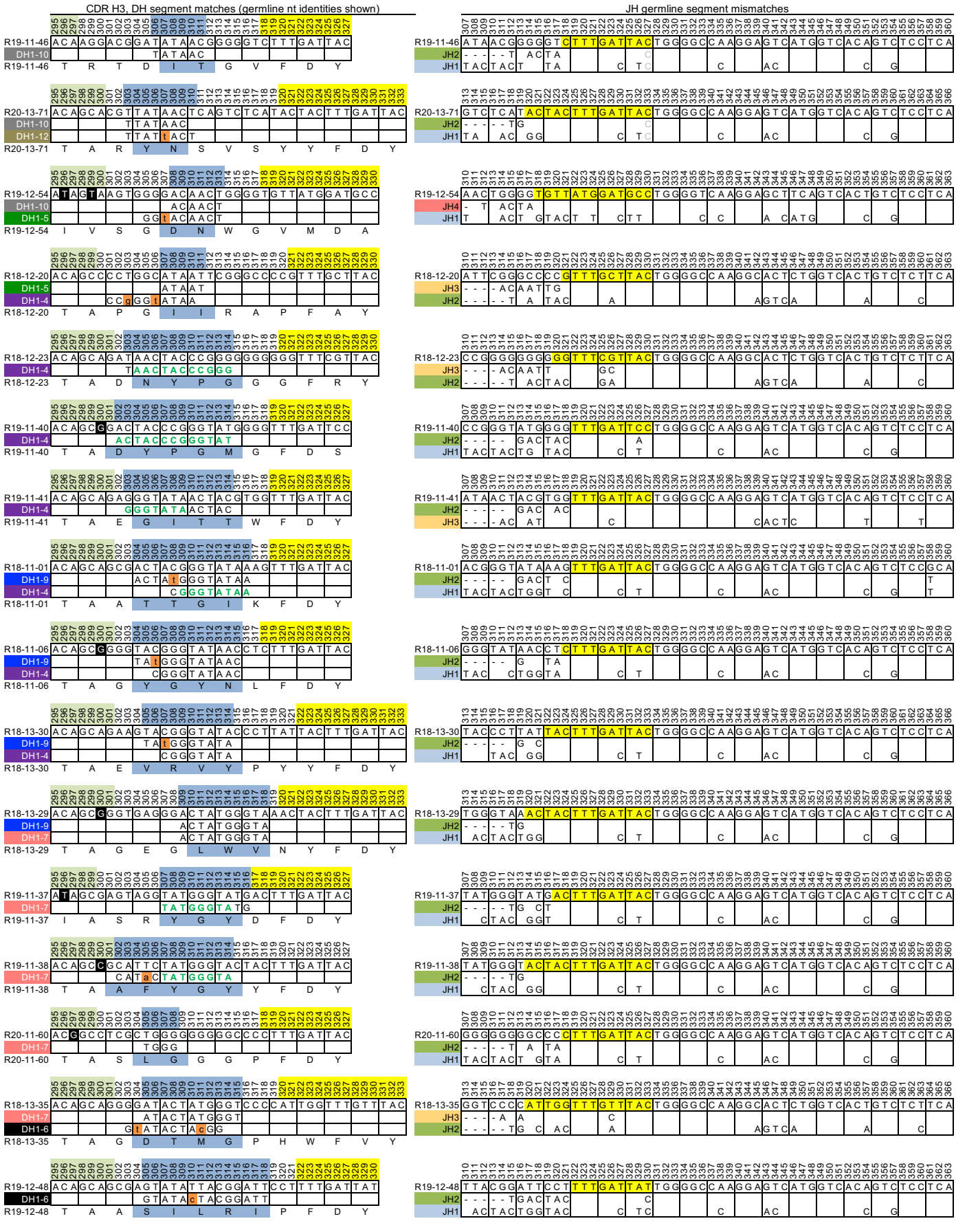
CDR H3, DH segment matches (germline nt identities shown)
JH germline segment mismatches
R19-11-46
DH1-10
R19-11-46
R20-13-71
DH1-10
DH1-12
R20-13-71
R19-12-54
DH1-10
DH1-5
R19-12-54
R18-12-20
DH1-5
DH1-4
R18-12-20
R18-12-23
DH1-4
R18-12-23
R19-11-40
DH1-4
R19-11-40
R19-11-41
DH1-4
R19-11-41
R18-11-01
DH1-9
DH1-4
R18-11-01
R18-11-06
DH1-9
DH1-4
R18-11-06
R18-13-30
DH1-9
DH1-4
R18-13-30
R18-13-29
DH1-9
DH1-7
R18-13-29
R19-11-37
DH1-7
R19-11-37
R19-11-38
DH1-7
R19-11-38
R20-11-60
DH1-7
R20-11-60
R18-13-35
DH1-7
DH1-6
R18-13-35
R18-12-48
DH1-6
R18-12-48
JH2
JH1
JH4
JH3

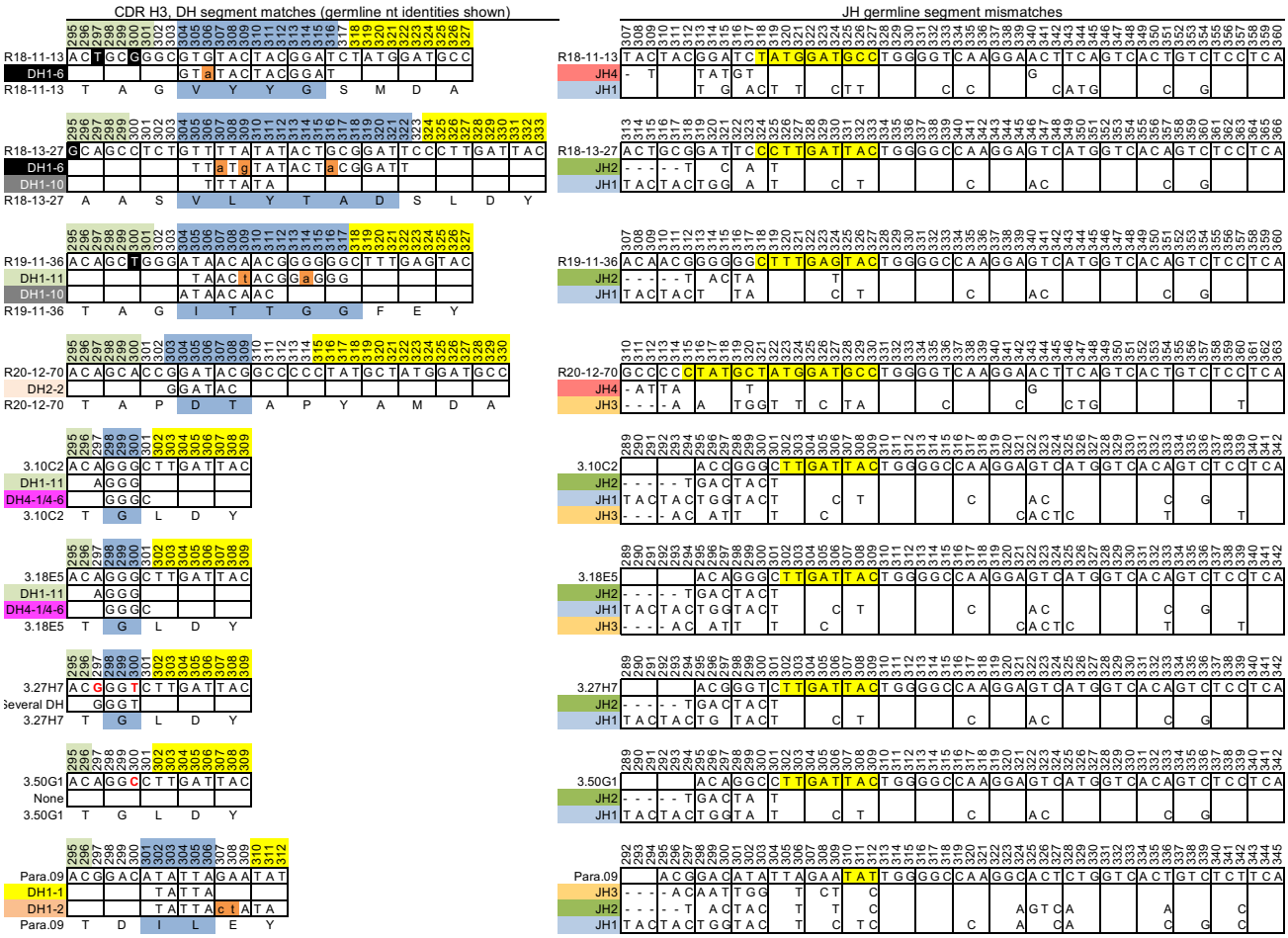
CDR H3, DH segment matches (germline nt identities shown)
JH germline segment mismatches
R18-11-13
DH1-6
R18-11-13
JH4
JH1
R18-13-27
DH1-6
DH1-10
R18-13-27
JH2
JH1
R19-11-36
DH1-11
DH1-10
R19-11-36
JH2
JH1
R20-12-70
DH2-2
R20-12-70
JH4
JH3
3.10C2
DH1-11
DH4-1/4-6
3.10C2
JH2
JH1
JH3
3.18E5
DH1-11
DH4-1/4-6
3.18E5
JH2
JH1
JH3
3.27H7
Several DH
3.27H7
JH2
JH1
3.50G1
None
3.50G1
JH2
JH1
Para.09
DH1-1
DH1-2
Para.09
JH3
JH2
JH1

VL junction

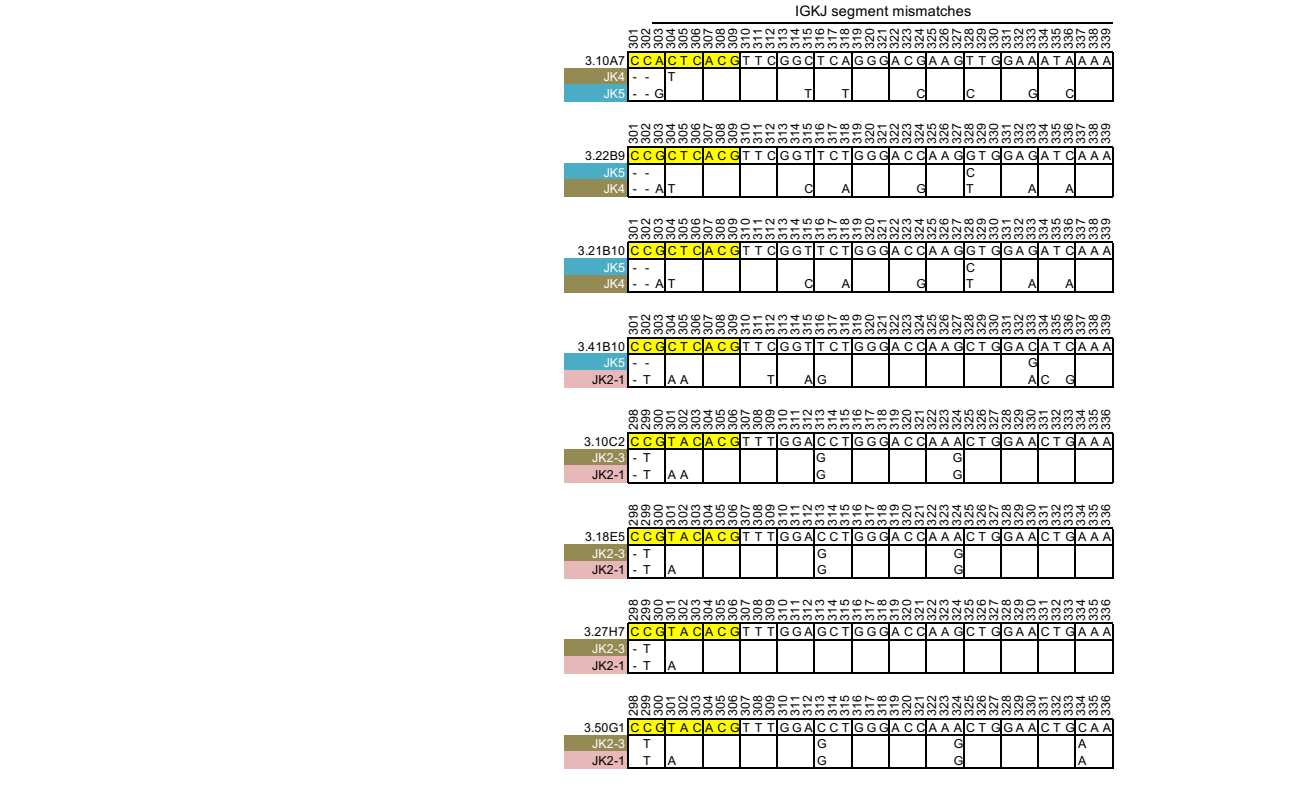
IGKJ segment mismatches
3.10A7
JK4
JK5
3.22B9
JK5
JK4
3.21B10
JK5
JK4
3.41B10
JK5
JK2-1
3.10C2
JK2-3
JK2-1
3.18E5
JK2-3
JK2-1
3.27H7
JK2-3
JK2-1
3.50G1
JK2-3
JK2-1

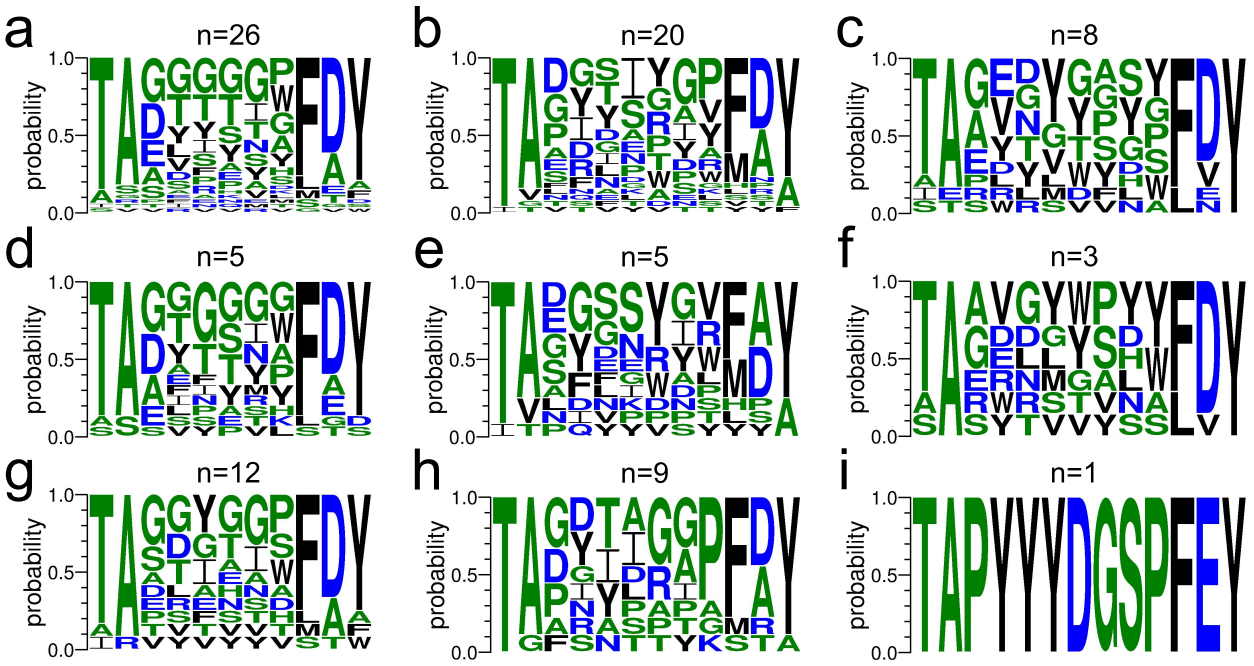


**Supplementary Fig. 4 CDR H3 consensus sequences of 3.10A7 $V_H$ parallel lineage clones.** Sequence logos for CDR H3 (combined IMGT® and Kabat definitions) with lengths 11 (panels a, d and g), 12 (b, e and h) and 13 (c, f, i) residues. Logos in panels a-c include CDR H3 sequences of clones that bound TREM2 peptide 139-148, shown in Figure 1. Logos in panels d-f include CDR H3 sequences of clones that did not bind TREM2. Logos in panels g-i include CDR H3 sequences of the strongest binders to TREM2 peptide 139-148 selected for pairing with additional light chains in Figure 1. The number of CDR H3 sequences in each Logo are indicated. CDR H3 sequences for each clones are listed in Supplementary File 1.

a

| Antibody | ka (1/Ms) | kd (1/s) | KD (M) |
|---|---|---|---|
| 3.10C2 | 3.2E+05 | 4.5E-05 | 1.4E-10 |
| 3.27H7 | 4.5E+05 | 6.7E-05 | 1.5E-10 |
| 3.18E5 | 3.0E+05 | 3.3E-05 | 1.1E-10 |
| 3.50G1 | 3.1E+05 | 2.0E-04 | 6.7E-10 |

b

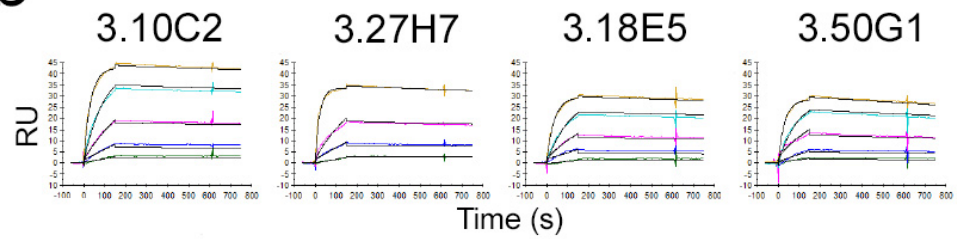


c

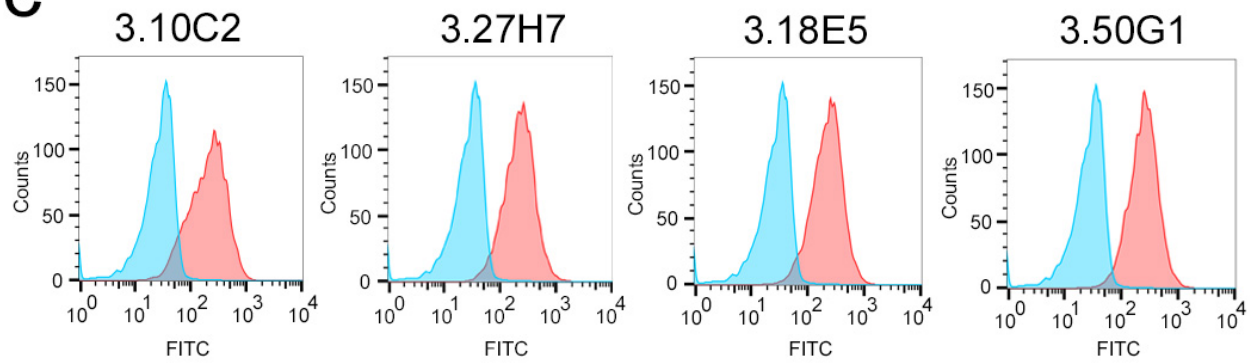


**Supplementary Fig. 5 Binding affinities of antibodies in the 3.10C2 clonal lineage.** (a) Monovalent binding kinetics and $K_D$ of antibodies to TREM2 at 37ºC by SPR measured in a Biacore T200 instrument. (b) SPR sensorgrams corresponding to kinetics data in panel (a). Color and black lines are sensorgram data and curve fitting, respectively. TREM2 antigen used at 100 nM for the highest concentration followed by 3-fold dilutions. (c) Binding of antibodies 3.10C2, 3.27H7, 3.18E5 and 3.50G1 recombinant antibodies to Jurkat cells expressing TREM2 by flow cytometry. Blue, control IgG2a. Red, anti-TREM2 antibodies. FITC, Fluorescein isothiocyanate gate.

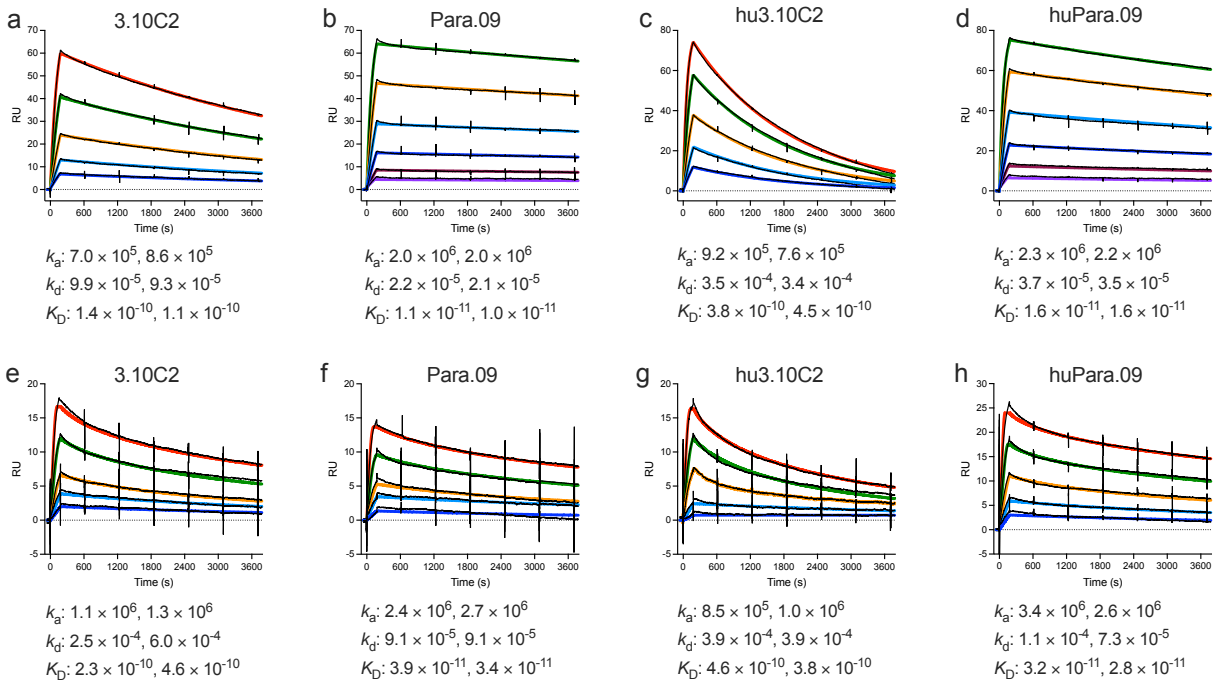


**Supplementary Fig. 6 SPR sensorgrams of anti-TREM2 antibodies binding to TREM2.** Sensorgrams correspond to binding kinetics data shown in Table 1. Representative sensorgrams for (a and e) 3.10C2, (b and f) Para.09, (c and g) hu3.10C2, and (d and h) huPara.09 binding to TREM2 at 37°C are shown. Panels e-h show sensorgrams for the same molecules as in panels a-d but at lower antibody capture densities. Each of the panels is a representative of two experiments at different antibody capture levels, with the kinetic data for each of the repeats shown below each sensorgram. The units for $k_a$, $k_d$, and $K_D$ values shown are $M^{-1}s^{-1}$, $s^{-1}$ and M, respectively. Sensorgram and fitted curves (1:1 model) are shown in black and colored lines, respectively. TREM2 concentrations used in panels a-d are 10 nM (red), 5 nM (green), 2.5 nM (orange), 1.25 nM (cyan), 0.625 nM (blue), 0.3125 nM (maroon), and 0.156 nM (purple), indicated in the corresponding fitted curves. TREM2 concentrations used in panels e-h are 7.5 nM (red), 3.75 nM (green), 1.875 nM (orange), 0.9375 nM (cyan) and 0.4688 nM (blue), indicated in the corresponding fitted curves. RU, response units.

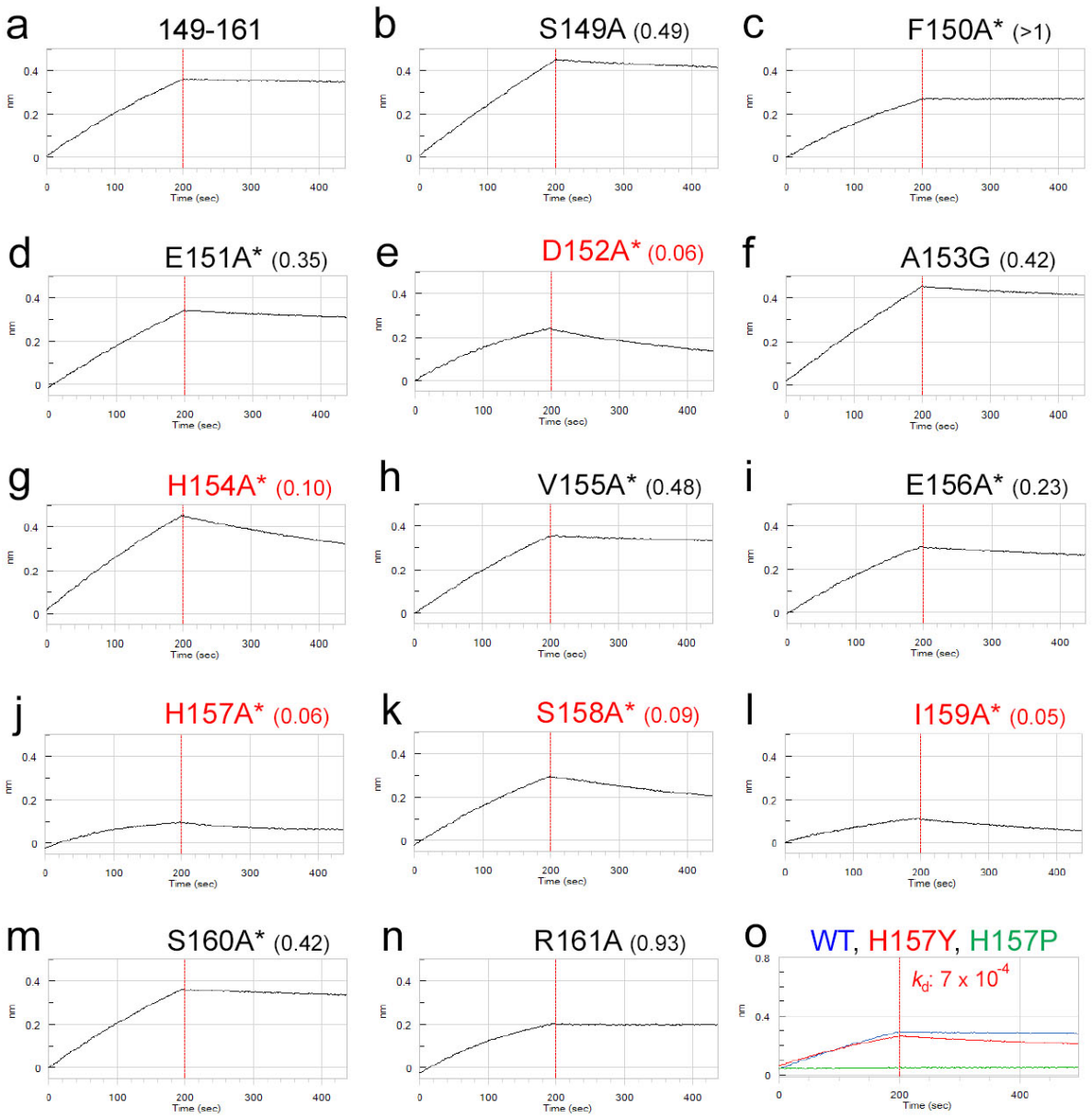


**Supplementary Fig. 7 Scanning mutagenesis of the TREM2 epitope bound by antibody 3.10C2.** Binding of 3.10C2 Fab fragments to wild-type (a, n) and indicated mutant TREM2 peptides (b-n) immobilized on sensor tips by biolayer interferometry (BLI). Red lines indicate change between Fab loading and dissociation steps. The ratios between the apparent dissociation rate of the wild-type 149-161 and mutant peptides are shown in parentheses. (o) Binding of 3.10C2 Fab fragments to wild-type, H157Y and H157P mutant peptides shown in blue, red and green, respectively. The apparent $k_d$ of the Fab with the H157Y mutant peptide is shown. All peptides encompass the TREM2 residues 149 to 161 with the indicated alanine, glycine or indicated mutations. Mutants indicated in red in panels b to n had a strong impact on apparent dissociation rates (ratio threshold set at < 0.20). Residues with side-chains at the binding interface are indicated with asterisks in panels b to n.

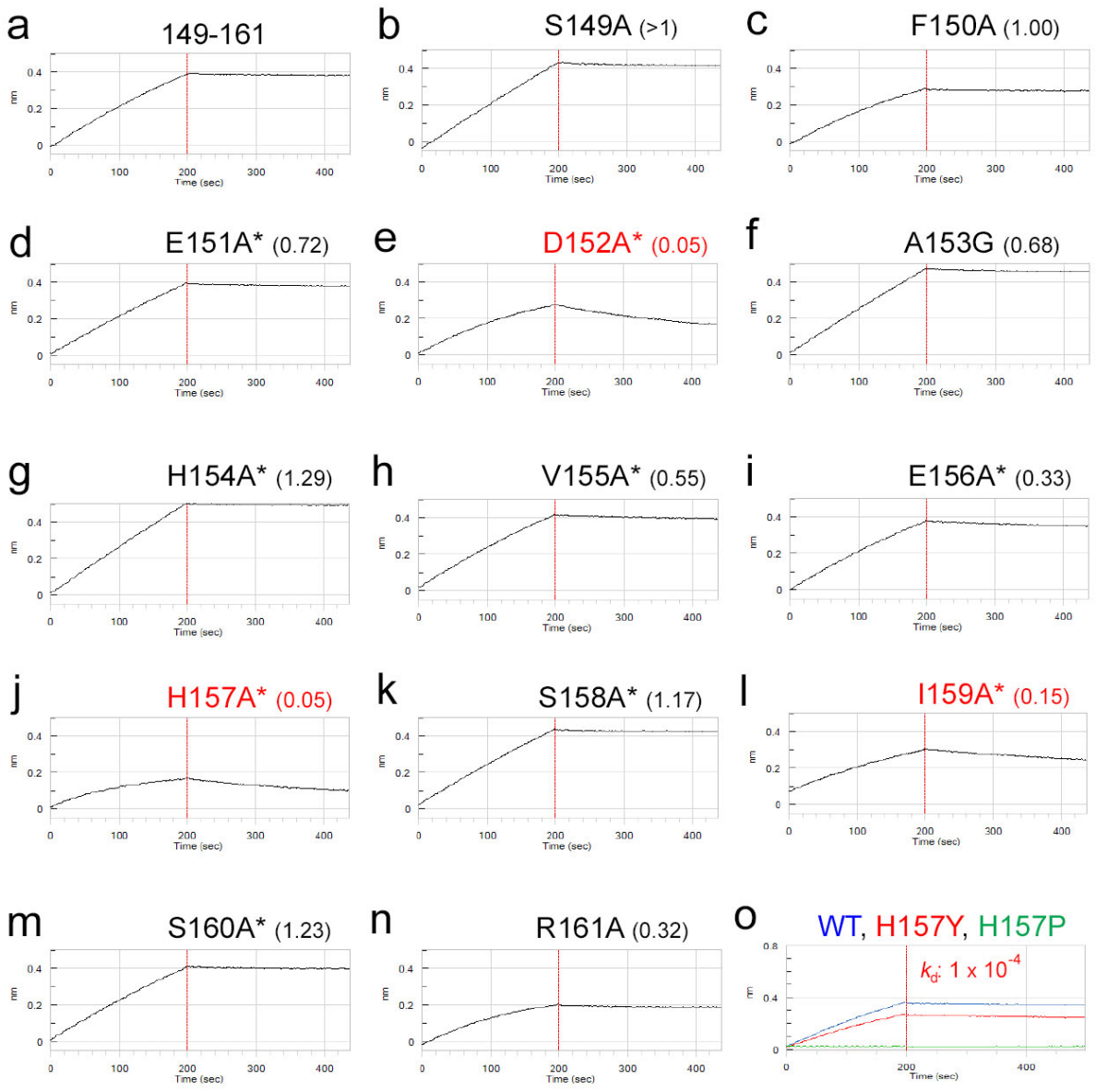


**Supplementary Fig. 8 Scanning mutagenesis of the TREM2 epitope bound by antibody Para.09.** Binding of Para.09 Fab fragments to wild-type (a, n) and indicated mutant TREM2 peptides (b-n) immobilized on sensor tips by biolayer interferometry (BLI). Red lines indicate change between Fab loading and dissociation steps. The ratios between the apparent dissociation rate of the wild-type 149-161 and mutant peptides are shown in parentheses. (o) Binding of Para.09 Fab fragments to wild-type, H157Y and negative control H157P mutant peptides shown in blue, red and green. The apparent $k_d$ of the Fab with the H157Y mutant peptide is shown. All peptides encompass the TREM2 residues 149 to 161 with the indicated alanine, glycine or indicated mutations. Mutants indicated in red in panels b to n had a strong impact on apparent dissociation rates (ratio threshold set at < 0.20). Residues with side-chains at the binding interface are indicated with asterisks in panels b to n.

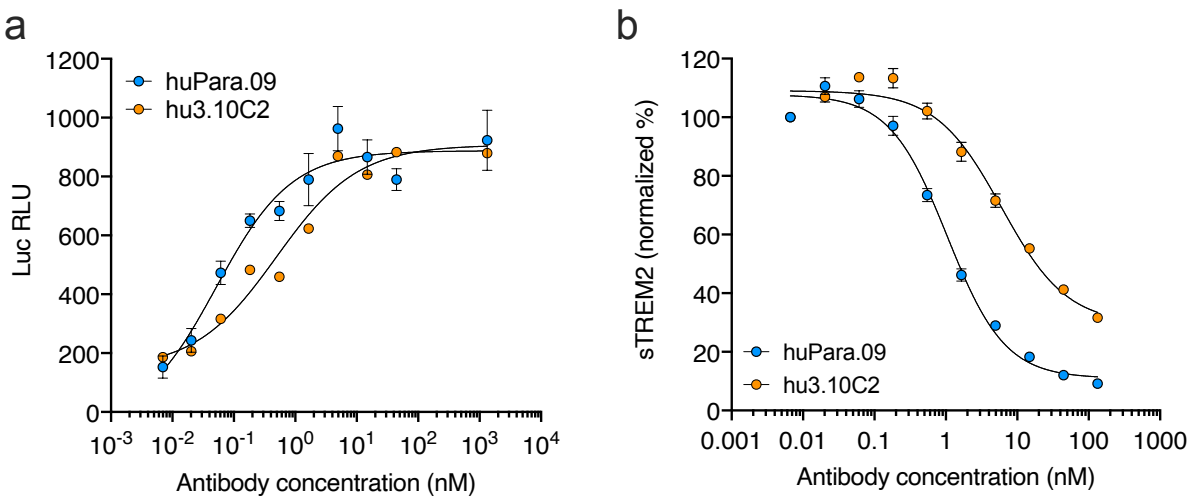


**Supplementary Fig. 9 Agonist and sTREM2 shedding blocking activity of humanized hu3.10C2 and huPara.09 antibodies.** (a) Agonist activity of humanized hu3.10C2 and huPara.09 antibodies in Jurkat-NFAT-TREM2-DAP12 cell reporter cells. (b) Blocking of TREM2 shedding into the supernatants of Jurkat cells expressing TREM2 by humanized hu3.10C2 and huPara.09, normalized to untreated cells. Error bars show standard deviation of n=3 repeats for each data point. Source data are provided as a Source Data file.

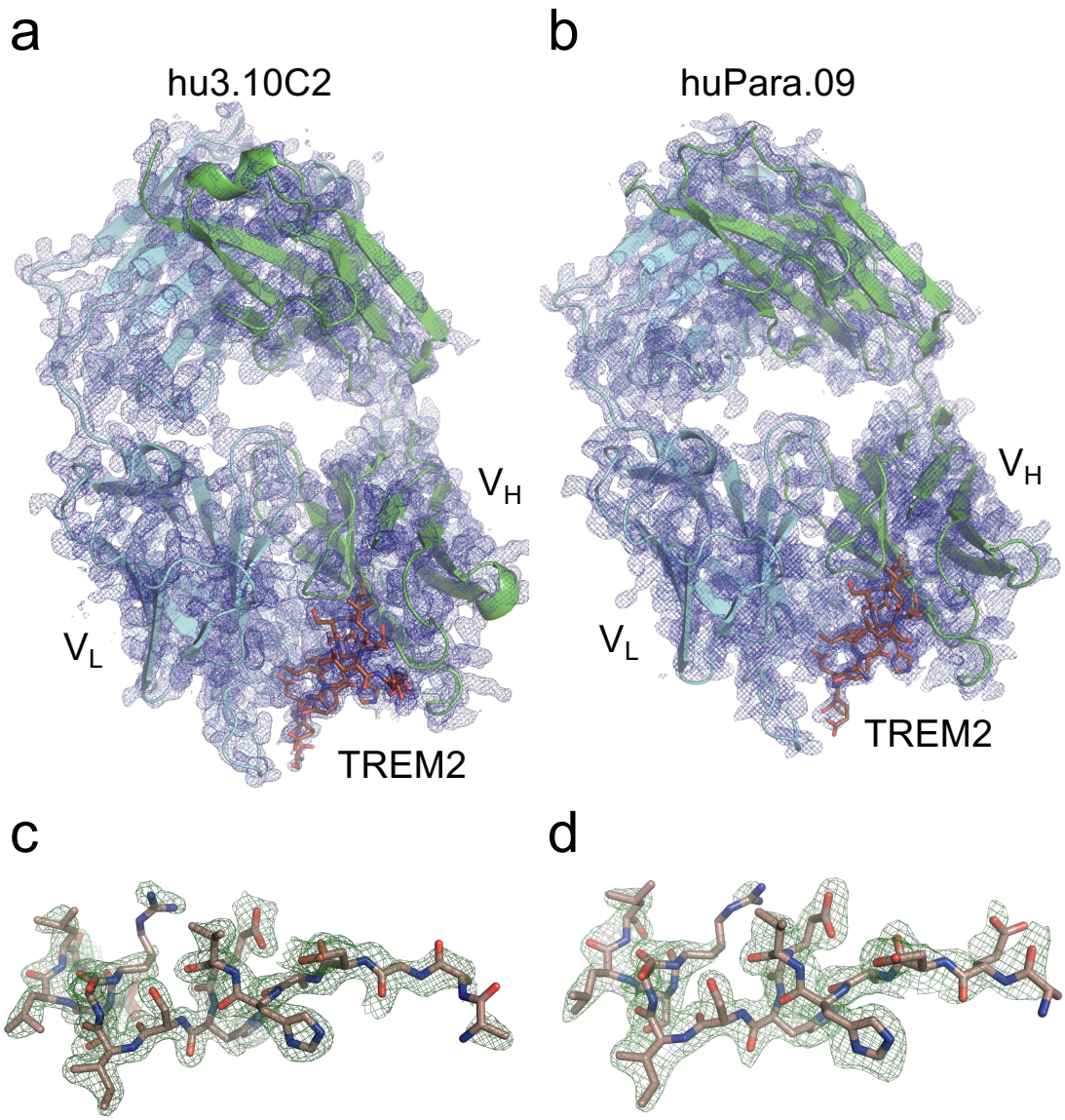


**Supplementary Fig. 10 Structures of anti-TREM2-TREM2 complexes and bound TREM2 peptides.** $2F_o$-$F_c$ densities of the 3.10C2-TREM2 (a) and Para.09-TREM2 (b) complexes contoured at 1.0 σ are shown with the heavy and light chains colored green and blue. Panels c and d show the $F_o$-$F_c$ densities of the TREM2 peptide ($^{149}$SFEDAHVEHSISRSLLE$^{165}$) bound to hu3.10C2 and huPara.09, respectively, calculated prior to modeling, contoured at 2.5 σ.

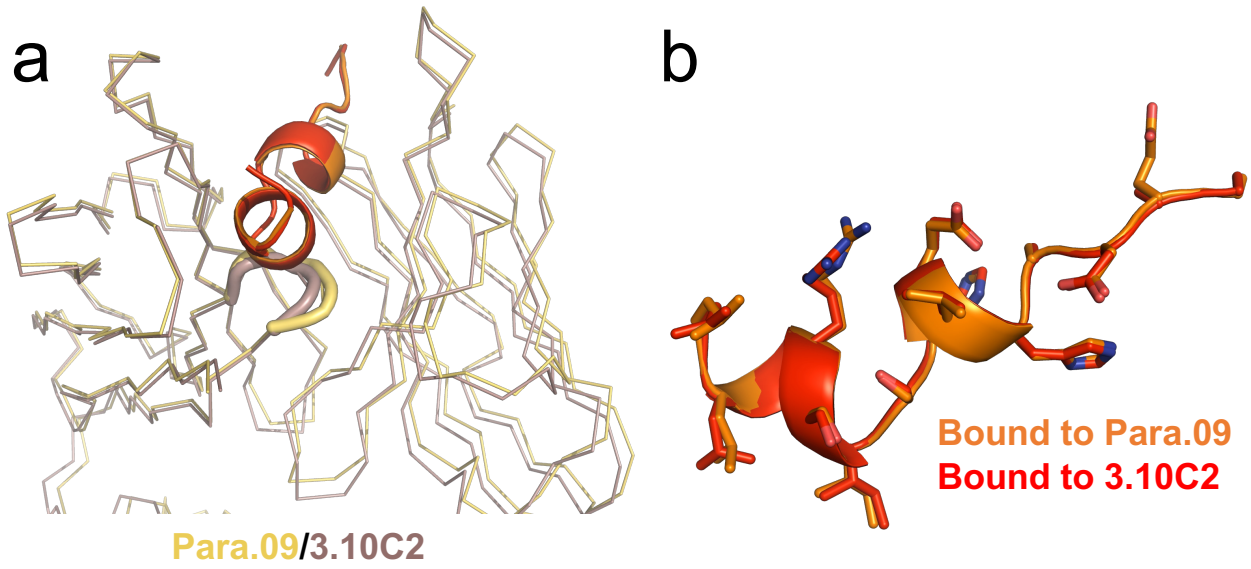


**Supplementary Fig. 11 Structural comparison of hu3.10C2-TREM2 and huPara.09-TREM2 complexes.** (a) Overall structure overlays of the Fab-peptide complexes aligned on the TREM2 peptide. The Fabs are shown in ribbon form with hu3.10C2 is shown in dark salmon and huPara.09 is in dark yellow. The hu3.10C2 and huPara.09 bound TREM2 peptides are shown in cartoon in red and orange respectively. CDR H3 is highlighted in tube form. (b) Close up view of the peptide conformation in both Fab contexts, with side chains shown as sticks. Color scheme is identical to panel a.

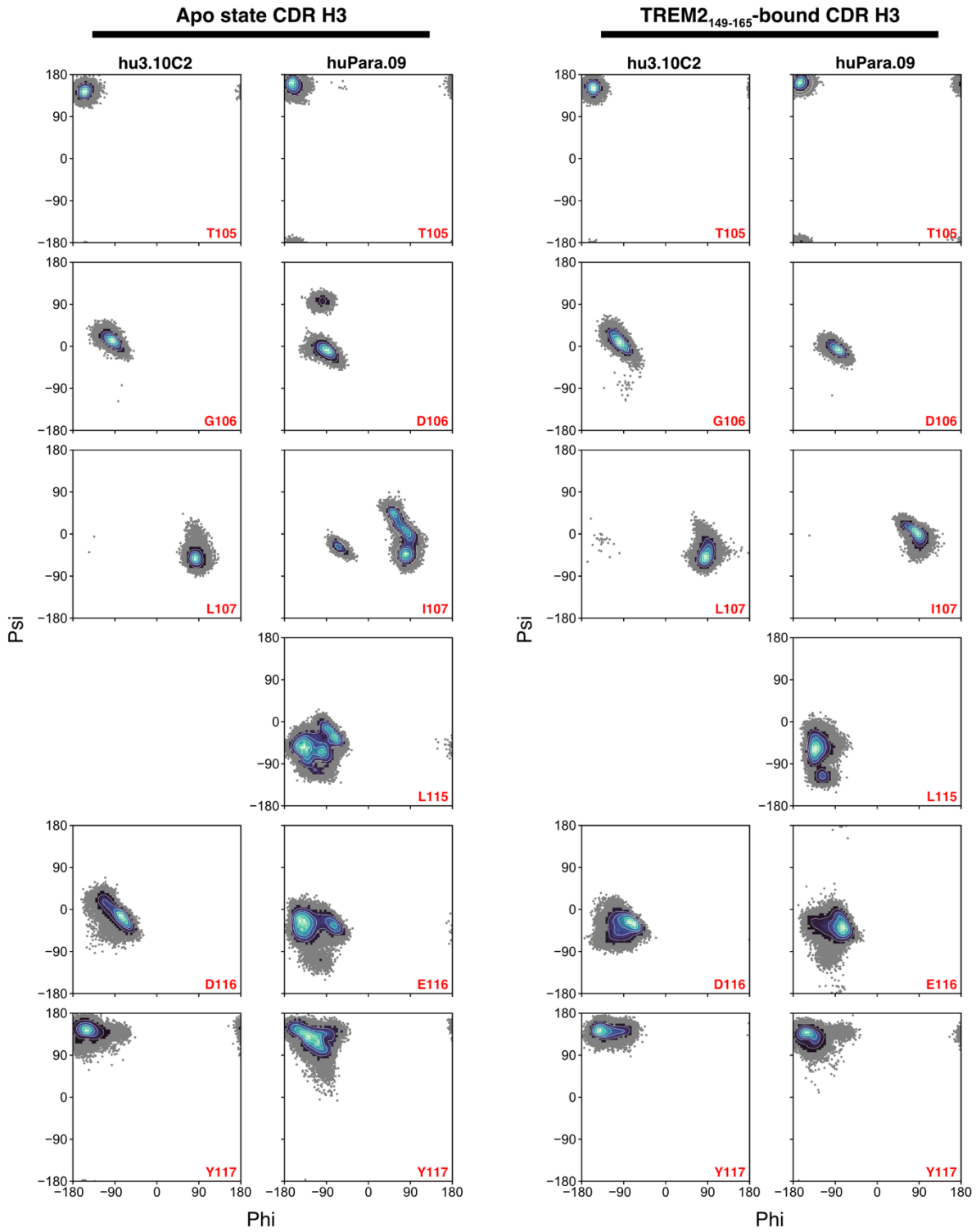


**Supplementary Fig. 12 Ramachandran plots of all residues in CDR H3.** All 3 independent simulations are considered in aggregate, with one point every 0.1 ns. Histogram bins are drawn only in regions with at least 10% of the total mass density. Contour lines are drawn every 20%.


**Supplementary Fig. 13 Ramachandran plots for all residues in TREM2.** Same as in Supplementary Figure 12, except for TREM2 residues. Magenta arrows indicate regions of Ramachandran space sampled by huPara.09-bound TREM2 that matches unbound states.

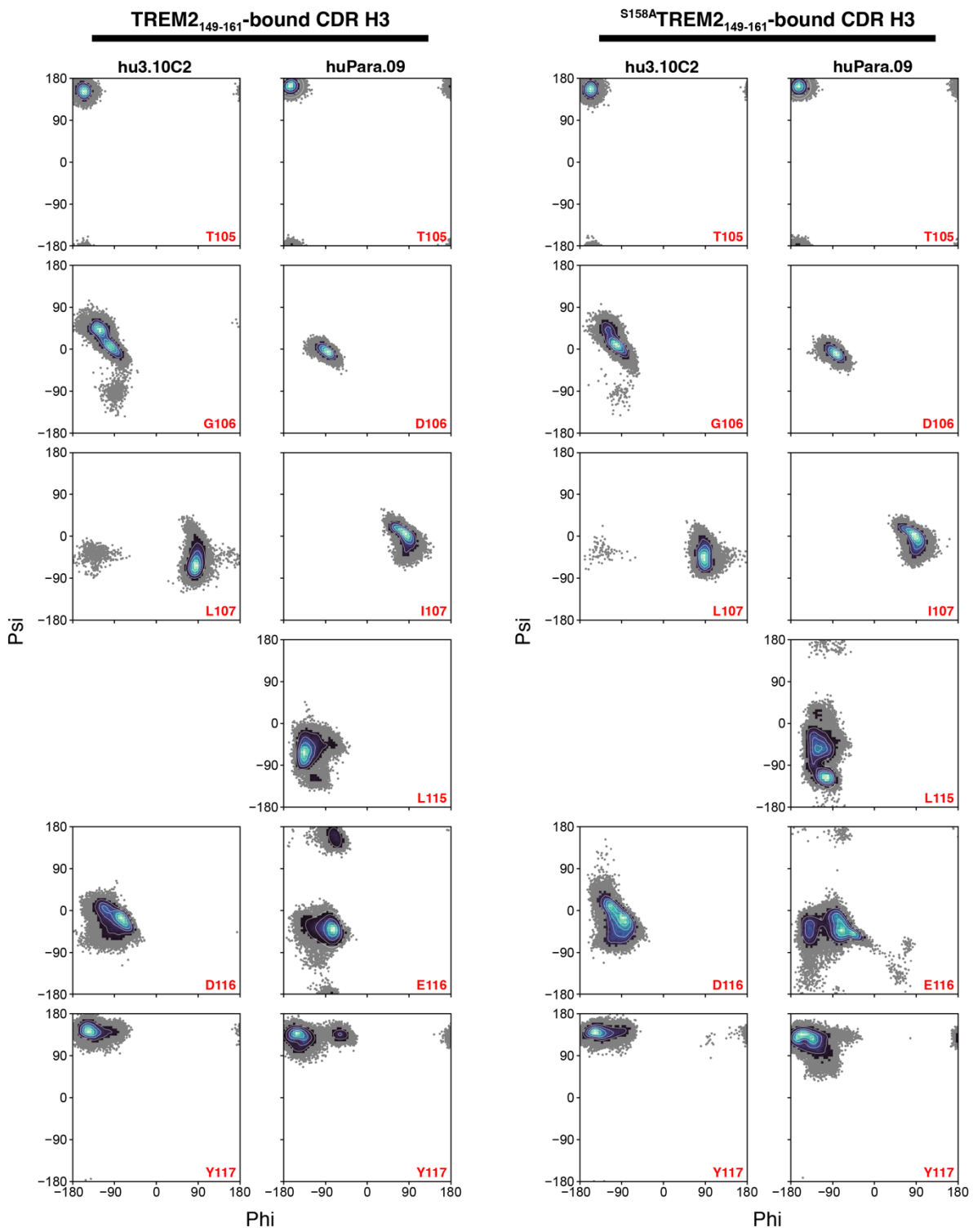


**Supplementary Fig. 14 Ramachandran plots of all residues in CDR H3 when bound to a truncated peptide.** Same as Supplementary Fig. 12, except for the peptide comprising TREM2 residues 149-161 (wild-type at left, S158A mutation at right).


**Supplementary Fig. 15 Ramachandran plots for all residues in truncated TREM2 peptide.** Same as in Supplementary Figure 13, except for the peptide comprising TREM2 residues 149-161 (wild-type).


**Supplementary Fig. 16 Ramachandran plots for all residues in truncated S158A TREM2 peptide.** Same as in Supplementary Figure 15, except for the S158A mutation of the peptide comprising TREM2 residues 149-161.

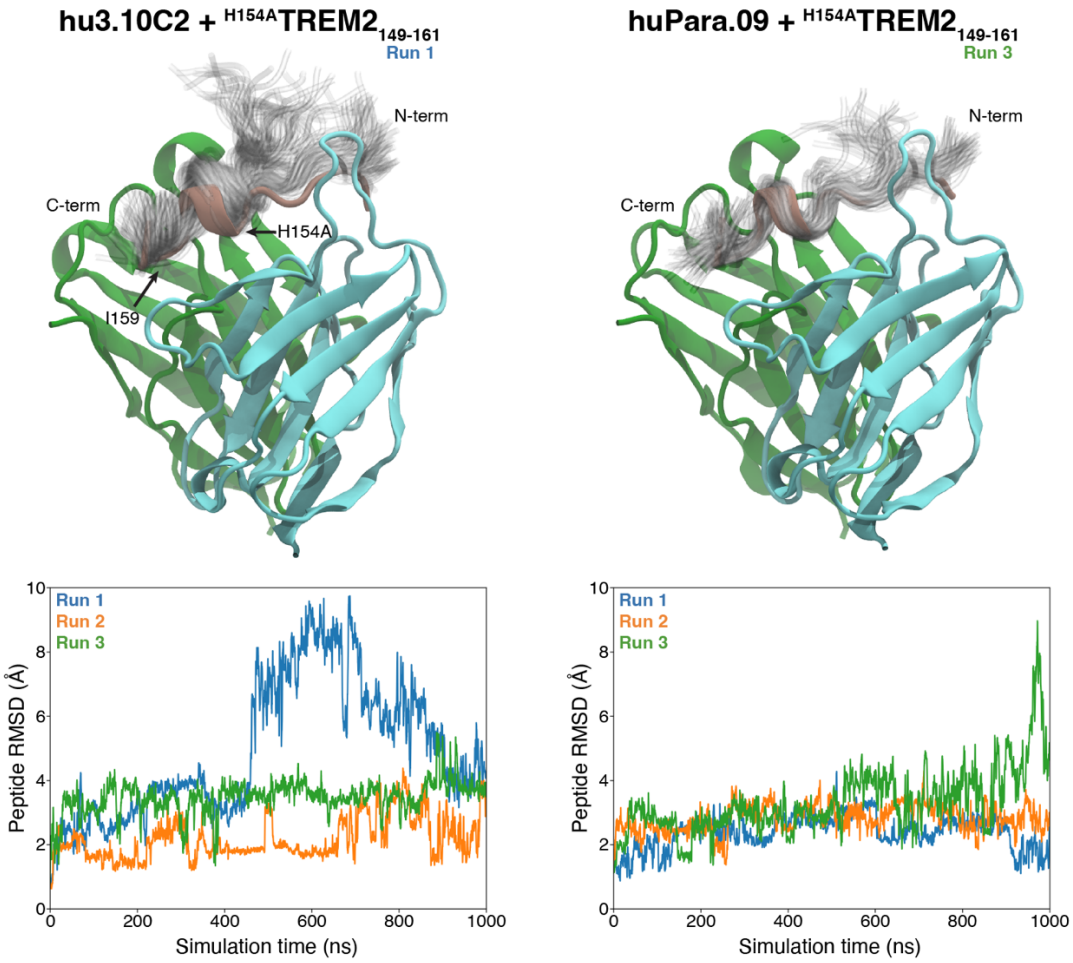


**Supplementary Fig. 17 Differential stability of the H154A mutant of the TREM2$_{149\text{-}161}$ peptide when bound to hu3.10C2 and huPara.09.** Renders as in Figure 7 are shown for the H154A mutant of the truncated peptide TREM2$_{149\text{-}161}$, reflecting the same experimental antigen as in Figure 2a, with peptide RSMD shown individually for each independent simulation run. The Figure shows simulations of mutant TREM2 bound to hu3.10C2 (left panels) and huPara.09 (right panels). The crystal structure (with TREM2 peptide manually truncated) is depicted in green (heavy), cyan (light), and brown (peptide), with snapshots every 10 ns of a 1 μs MD simulation in transparent tube after alignment of the antibody variable regions to the crystallographic coordinates. Below, the RMSD of the entire peptide over the course of each independent simulation is shown, using a 1 ns smoothed rolling window. The renders above are selected to be the most dynamic of the replicate simulations, and are indicated under the titles. Increased flexibility at the N-terminal half of the peptide is visible for both antibodies, though hu3.10C2 exhibits more dramatic unfolding and a larger displacement of the peptide's helical turn away from the crystallographic conformation, at times remaining anchored almost entirely by residue I159.

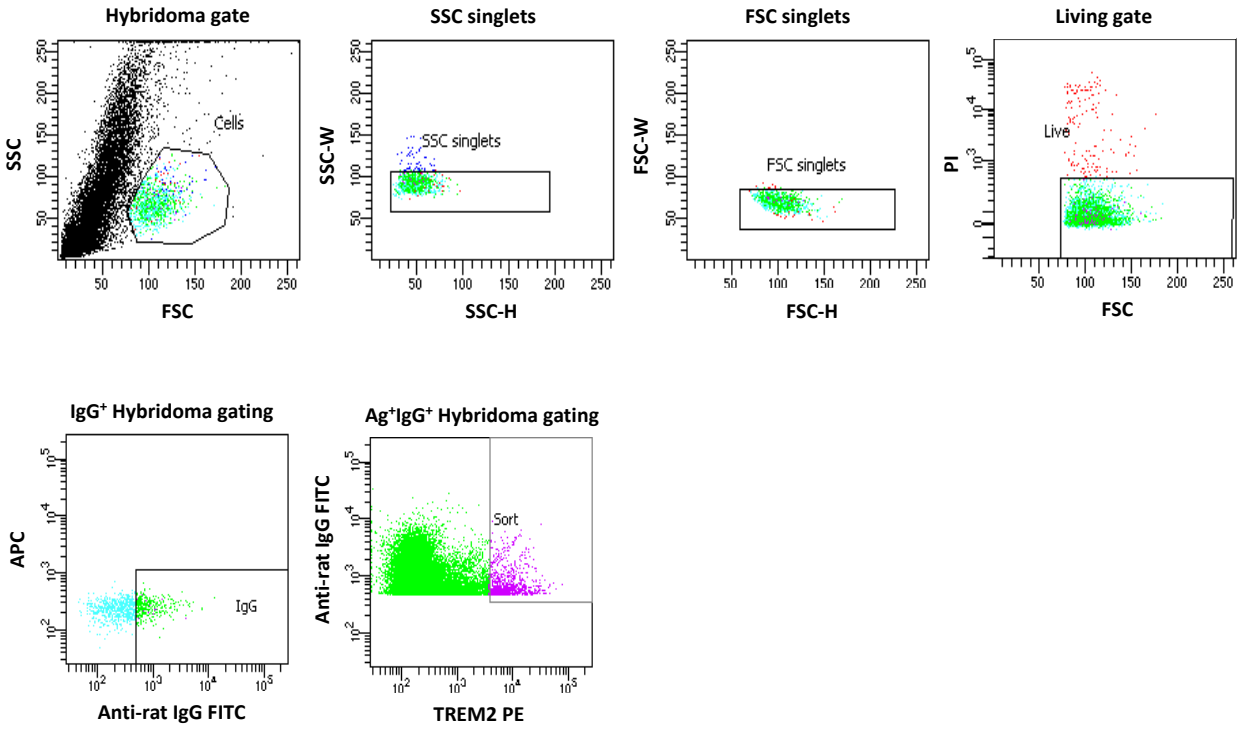


**Supplementary Fig. 18 Gating strategy for hybridoma cell selection.** Gating order is shown from left to right, top to bottom in the figure. Selected gates are delimited in boxes and lines. Single cells were identified by plotting SSC-H (side scatter pulse height) versus SSC-W (side scatter pulse width), and FSC-H (forward scatter pulse height) vs. FSC-W (forward scatter pulse width). Live cells were gated after excluding dead cells with Propidium Iodide (PI), $IgG^+$ hybridoma cells were initially gated using anti-rat IgG FITC, followed by the identification of $TREM2^+IgG^+$ hybridoma cells in subsequent gating. APC, unlabeled channel used only for dot plot display for sorting.

**Supplementary Table 1 – Data collection and refinement statistics (molecular replacement)**

| | huPara.09:TREM2 (PDB 8T59) | hu3.10C2:TREM2 (PDB 8T51) |
|---|---|---|
| **Data collection** | | |
| Space group | $P2_1\,2_1\,2_1$ | $P\,2\,2_1\,2_1$ |
| Cell dimensions | | |
| *a*, *b*, *c* (Å) | 54.17, 68.16, 254.79 | 66.38, 96.03, 144.32 |
| $\alpha, \beta, \gamma$ (°) | 90, 90, 90 | 90, 90, 90 |
| Resolution (Å) | 33.78-2.0(2.07-2.0) | 38.9-1.9(1.97-1.9) |
| $R_{sym}$ or $R_{merge}$ | 0.1165(1.72) | 0.122(1.495) |
| $I / \sigma I$ | 11.70(1.00) | 12.98(1.88) |
| Completeness (%) | 99.89(99.99) | 99.93(100.00) |
| Redundancy | 6.3(6.6) | 6.7(6.9) |
| | | |
| **Refinement** | | |
| Resolution (Å) | 34.08-2.0 | 38.9-1.9 |
| No. reflections | 73218 | 73390 |
| $R_{work}$ / $R_{free}$ | 0.2051/0.2399 | 0.1928/0.2404 |
| No. atoms | 7534 | 7615 |
| Protein | 6874 | 6916 |
| Ligand/ion | 164 | 277 |
| Water | 586 | 549 |
| *B*-factors | | |
| Protein | 35.5 | 31.2 |
| Ligand/ion | 53.4 | 56.77 |
| Water | 39.8 | 36.93 |
| R.m.s. deviations | | |
| Bond lengths (Å) | 0.007 | 0.011 |
| Bond angles (°) | 1.23 | 1.30 |

## Supplementary Table 2 – Hydrogen bond distances between antibodies and TREM2

| Para09_L46 | | | | | | | | | |
|---|---|---|---|---|---|---|---|---|---|
| **TREM2** | **LC** | **Type** | **Interaction** | **Distance (Å)** | **HC** | **Type** | **Interaction** | **Distance** | **Comments** |
| Glu148 | | | | | | | | | |
| Ser149 | | | | | | | | | |
| Phe150 | | | | | | | | | |
| Glu151 | | | | | | | | | |
| Asp152 | Ser37, Tyr39, Arg 55 | H-bond | Asp152(SC)-Ser37(SC),Tyr39(SC),Arg55(SC) | 2.8 (Ser37), 2.6 (Tyr39), 2.9 (Arg55) | | | | | |
| Ala153 | | | | | | | | | |
| His154 | Phe96, Tyr101 | H-bond | His154-Phe96(BB),Tyr101(SC) | 2.9 (Phe96), 3.1 (Tyr101) | His35 | H-bond, indirect | His154(SC)-H2O-His35(SC) | 2.9 (His154-H2O), 2.8 (H2O-His35) | His154 sits in a hydrophobic pocket formed by LC-Tyr39, Phe96, Tyr101, HC-Trp33, His35, His50, Ile101, Leu102. Surface is complementary but too far for direct contact. |
| Val155 | Tyr54, Arg55 | hydrophobic | Val155(SC)-Tyr54(SC), Arg55(SC) | 4.1 (Tyr54), 3.5 (Arg55) | | | | | Arg55 is neutralized by TREM2-Glu156 allowing for hydrophobic interaction with Val155. |
| Glu156 | Arg55 | salt bridge | Glu156(SC)-Arg55(SC) | 2.9 | | | | | |
| His157 | | | | | Trp33 | stacking | His157(SC)-Trp33(SC) | 3.4 | His157 appears to coordinate a zinc using the imidazole ring. Likely a crystallization artifact as mutation of His157 does not disrupt interaction. |
| Ser158 | | | | | | | | | |
| Ile159 | | | | | Val2, Leu4, Phe27, Val32, Asp100, Tyr104 | hydrophobic, H-bond | Ile159(SC)-Val2(SC), Leu4(SC), Phe27(SC), Val32(SC), Tyr104(SC) Ile159(BB)-Asp100(SC) | 4.1 (Val2), 4.2 (Leu4), 3.7 (Phe27), 3.7 (Val32), 2.8 (Asp100), 3.7 (Tyr104) | HC forms a perfect hydrophobic cage to enclose TREM2-Ile159 within. Replacement of Met34-->Leu in Para09 likely increases hydrophobic nature of pocket. Asp100(SC) interaction is unique to Para09. |
| Ser160 | | | | | Glu103, Tyr104 | H-bond | Ser160(SC)-Glu103(SC) | 2.9 (Glu103) | |
| Arg161 | | | | | | | | | |
| Ser162 | | | | | | | | | |
| Leu163 | | | | | Val2 | hydrophobic | Leu163(SC)-Val2(SC) | 4 | Leu163(SC) sits on top of a shallow cleft formed by HC-Val2, Phe27, Tyr104 |
| Leu164 | | | | | | | | | |
| Glu165 | | | | | | | | | |
| | | | | | | | | | |
| **3.10C2_L46** | | | | | | | | | |
| **TREM2** | **LC** | **Type** | **Interaction** | | **HC** | **Type** | **Interaction** | | |
| Glu148 | | | | | | | | | |
| Ser149 | Leu97 | H-bond | Ser149(BB)-Leu97(BB) | 3.2 | | | | | |
| Phe150 | | | | | | | | | |
| Glu151 | | | | | | | | | |
| Asp152 | Ser37, Tyr39, Arg 55 | H-bond | Asp152(SC)-Ser37(SC),Tyr39(SC),Arg55(SC) | 2.6 (Ser37), 3.2 (Tyr39), 2.8 (Arg55) | | | | | |
| Ala153 | | | | | | | | | |
| His154 | Phe96, Tyr101 | H-bond | His154-Phe96(BB),Tyr101(SC) | 2.7 (Phe96), 3.1 (Tyr101) | His35, His50 | H-bond, indirect | His154(SC)-H2O-His35(SC) His154(SC)-H2O-His50(SC) | 2.8 (His154-H2O), 2.8 (H2O-His35), 3.3 (H2O-His50) | His154 sits in a hydrophobic pocket formed by LC-Tyr39, Phe96, Tyr101, HC-Trp33, His35, His50, Leu101. Cavity is less "deep" compared to Para09. |
| Val155 | Tyr54, Arg55 | hydrophobic | Val155(SC)-Tyr54(SC), Arg55(SC) | 3.7 (Tyr54), 3.5 (Arg55) | | | | | Arg55 is neutralized by TREM2-Glu156 allowing for hydrophobic interaction with Val155. |
| Glu156 | Arg55 | salt bridge | Glu156(SC)-Arg55(SC) | 3 | | | | | |
| His157 | | | | | Trp33 | stacking | His157(SC)-Trp33(SC) | 3.3 | His157 appears to coordinate a zinc using the imidazole ring. Likely a crystallization artifact as mutation of His157 does not disrupt interaction. |
| Ser158 | | | | | | | | | |
| Ile159 | | | | | Val2, Leu4, Phe27, Val32, Met34, Tyr104 | hydrophobic | Ile159(SC)-Val2(SC), Leu4(SC), Phe27(SC), Val32(SC), Met34(SC), Tyr104(SC) | 3.8 (Val2), 4.2 (Leu4), 3.8 (Phe27), 3.7 (Val32), 4.1 (Met34), 3.8 (Tyr104) | HC forms a perfect hydrophobic cage to enclose TREM2-Ile159 within. |
| Ser160 | | | | | Asp102 | H-bond | Ser160(SC)-Asp102(SC) | 2.5 | |
| Arg161 | | | | | | | | | |
| Ser162 | | | | | | | | | |
| Leu163 | | | | | | | | | |
| Leu164 | | | | | | | | | |
| Glu165 | | | | | | | | | |

SC: side-chain; BB: backbone

**Supplementary Table 3 – Two body interaction energies between CDR H3 and all TREM2 residues for both the full 149–165 crystallized and truncated 149–161 peptides**

| Full-length TREM2 peptide (149 - 165) from complex structure | | | |
|---|---|---|---|
| Residue | hu3.10C2 CDR H3 | Residue | huPara.09 CDR H3 |
| T105 | -0.009659[a] | T105 | -0.001697 |
| G106 | -0.970836 | D106 | -6.471206 |
| L107 | -1.409727 | I107 | -1.131378 |
| - | - | L115 | -2.692249 |
| D116 | -7.185974 | E116 | -1.230671 |
| Y117 | -3.301817 | Y117 | -4.008381 |
| Total | -12.868354 | Total | -15.535582 |
| Energy / residue | -2.573671 | Energy / residue | -2.589264 |
| Short TREM2 peptide (149 - 161) from Ala-scan binding experiments | | | |
| Residue | hu3.10C2 CDR H3 | Residue | huPara.09 CDR H3 |
| T105 | -0.009659 | T105 | -0.001697 |
| G106 | -0.970836 | D106 | -6.471206 |
| L107 | -1.409727 | I107 | -1.131378 |
| - | - | L115 | -2.692249 |
| D116 | -7.185974 | E116 | -1.230671 |
| Y117 | -2.954668 | Y117 | -3.355351 |
| Total | -12.530864 | Total | -14.882552 |
| Energy / residue | -2.506173 | Energy / residue | -2.480425 |

[a] Rosetta Energy Units

**Supplementary Table 4 – Change in total two-body interaction energy between TREM2 and nearby antibody contacts upon computational alanine scanning**

| Mutation | hu3.10C2 | huPara.09 |
|---|---|---|
| S149A | −0.289370[a] | −1.892457 |
| F150A | −0.007318 | 0.072029 |
| E151A | 1.733891 | 0.153330 |
| D152A | 7.358706 | 6.864962 |
| A153A | 0.007399 | 0.006808 |
| H154A | 5.207345 | 4.535309 |
| V155A | 2.314930 | 2.803780 |
| E156A | 4.067127 | 4.310636 |
| H157A | 0.498704 | 0.507335 |
| S158A | −0.593746 | −0.516863 |
| I159A | 8.531770 | 8.675364 |
| S160A | 1.679109 | 0.030958 |
| R161A | −0.030632 | −0.067745 |
| H157Y | −2.058792 | −2.299264 |

[a] Rosetta Energy Units